3D Geometry and Hydrodynamics of Flares observed with EUVI

Markus J. Aschwanden
(LMSAL)

STEREO Science Working Group Meeting
Observatoire de Paris - Meudon - 20-22 April 2008
Session "Coronal/CMEs/Flares"
http://www.lmsal.com/~aschwand/ppt/2008_STEREO_Paris_MJA.ppt

STEREO/EUVI Observations of Flares (2007)

EUVI event catalog (http://secchi.lmsal.com/EUVI/work_euvi.txt)
-178 flare events >C1 GOES class or >25 keV (RHESS)
(Dec 2006-Jan 2008)
0 X-class flares
10 M-class flares
78 C-class flares

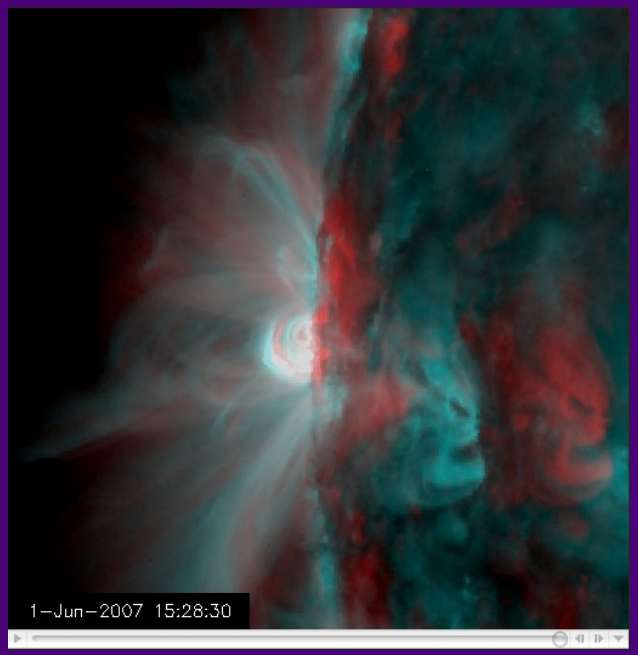

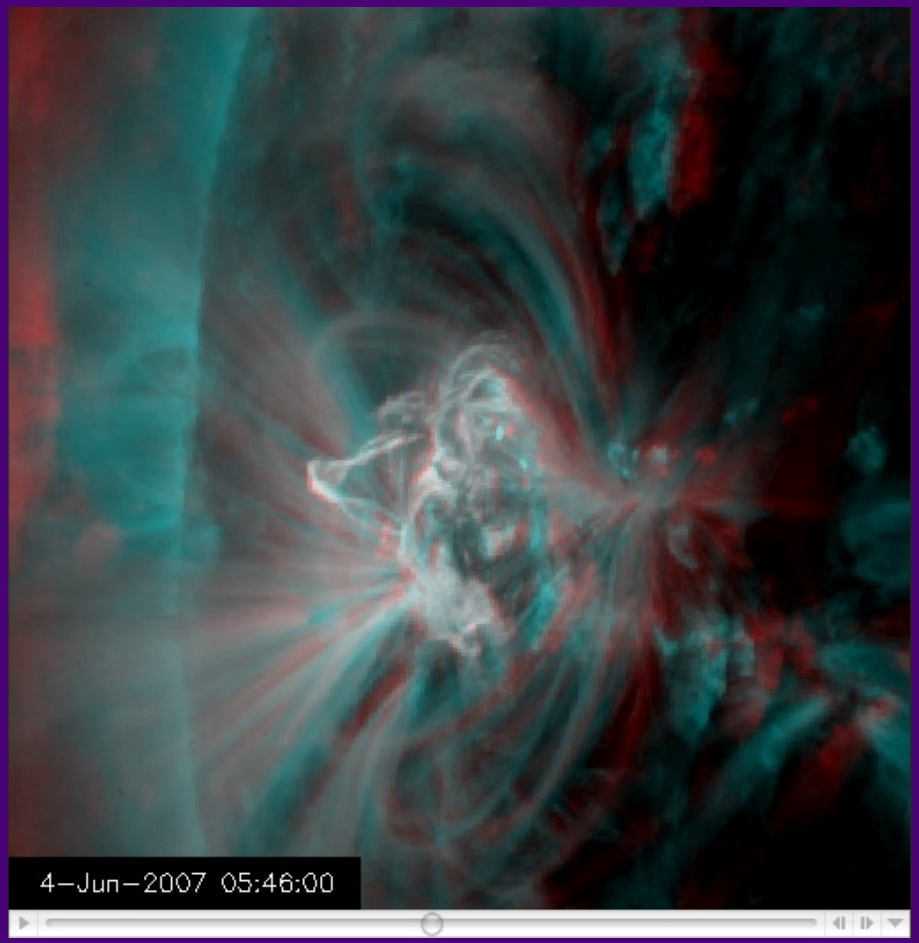

10 GOES M-Class Flares observed with EUVI

#	DATE	START	END	POSITION	CAD	GOES	RHESSI	LASCO	COR1	Occ
054	2007-Jun-01	06:40	07:40	S05E90	150	M1		LASCO	COR1	OCC
055	2007-Jun-01	14:30	15:30	S07E87	150	M2.8	12-25			OCC
059	2007-Jun-01	21:35	22:35	S07E82	150	M2.1	50-100	LASCO	COR1	OCC
060	2007-Jun-02	05:20	06:50	S08E87	150	M2.5	25-50	LASCO		
063	2007-Jun-02	10:20	11:20	S05E74	150	M1	25-50			
067	2007-Jun-03	01:40	02:06	S07E68	150	M2.4	12-25			
068	2007-Jun-03	02:06	02:30	S07E68	150	M7	12-25			
071	2007-Jun-03	06:30	08:10	S04E63	150	M4.5	12-25		COR1	
078	2007-Jun-04	05:00	06:30	S05E50	150	M8.9	12-25	LASCO		
104	2007-Jun-09	13:20	14:40	S10W23	150	M1	12-25	LASCO		

All flares originate from same active region during its transit from East 90 to West 23.

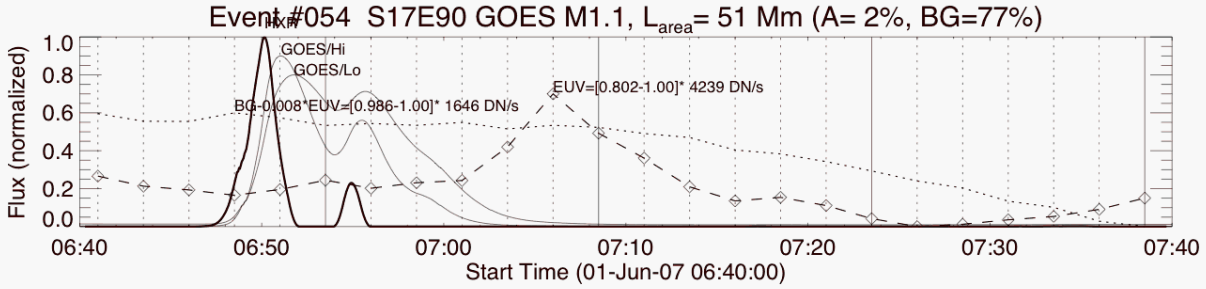

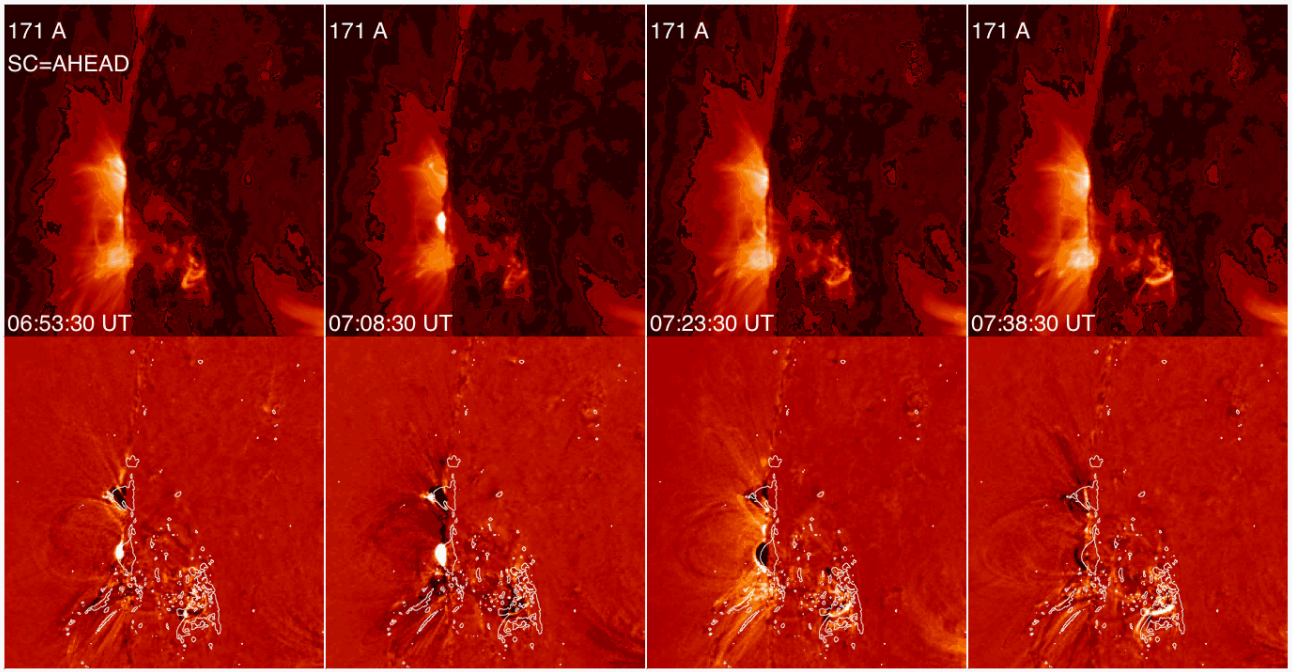

GOES/Hi 0.5-4 A
GOES/Lo 1-8 A
HXR~dF$_{GOES}$/dt
(RHESSI>25 keV)
EUVI 171 A
EUVI Backgr

EUVI 171 A

EUVI 171 A
Running difference

Event #54: 2007-Jun-01 14:40 UT
- occulted flare
- EUV peaks 20 min after SXR

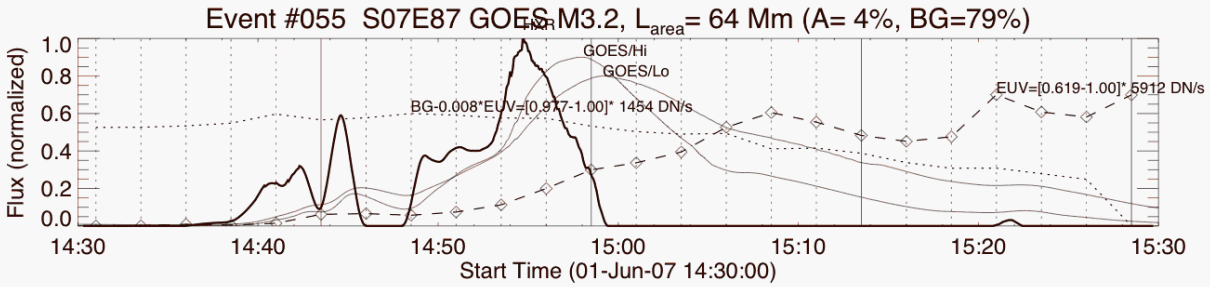

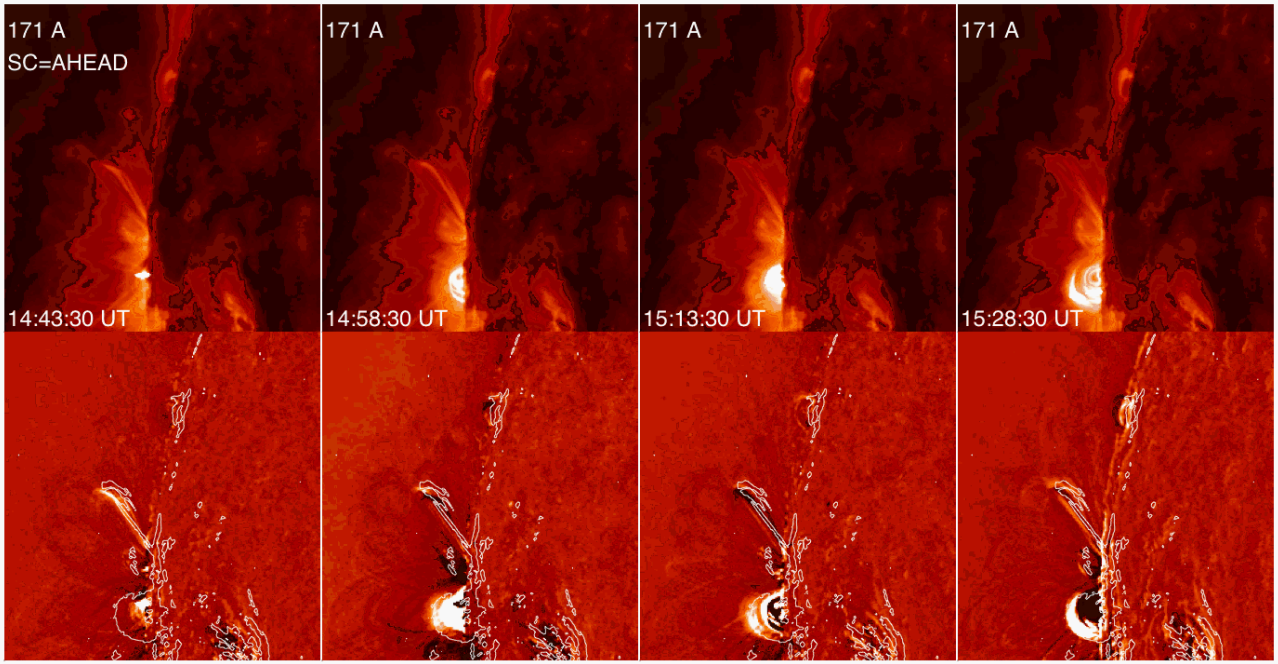

GOES/Hi 0.5-4 A
GOES/Lo 1-8 A
HXR~dF_{GOES}/dt
(RHESSI>25 keV)
EUVI 171 A
EUVI Backgr

EUVI 171 A

EUVI 171 A
Running difference

Event #55: 2007-Jun-01 14:40 UT
- occulted flare
- EUV increasing after SXR, peaks 8 min & 20 min later

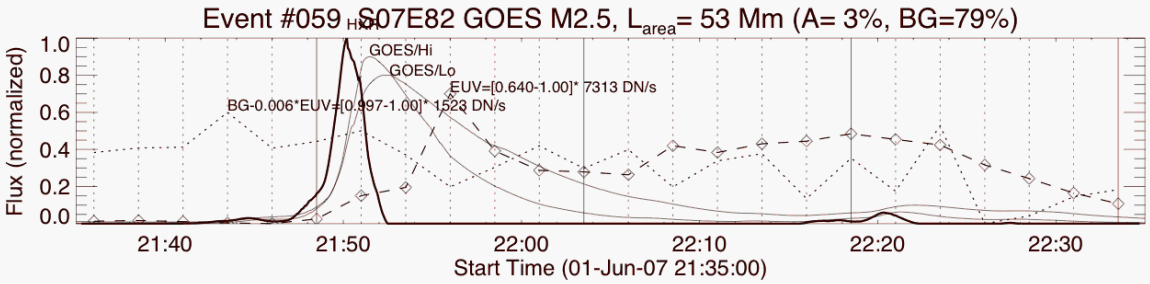

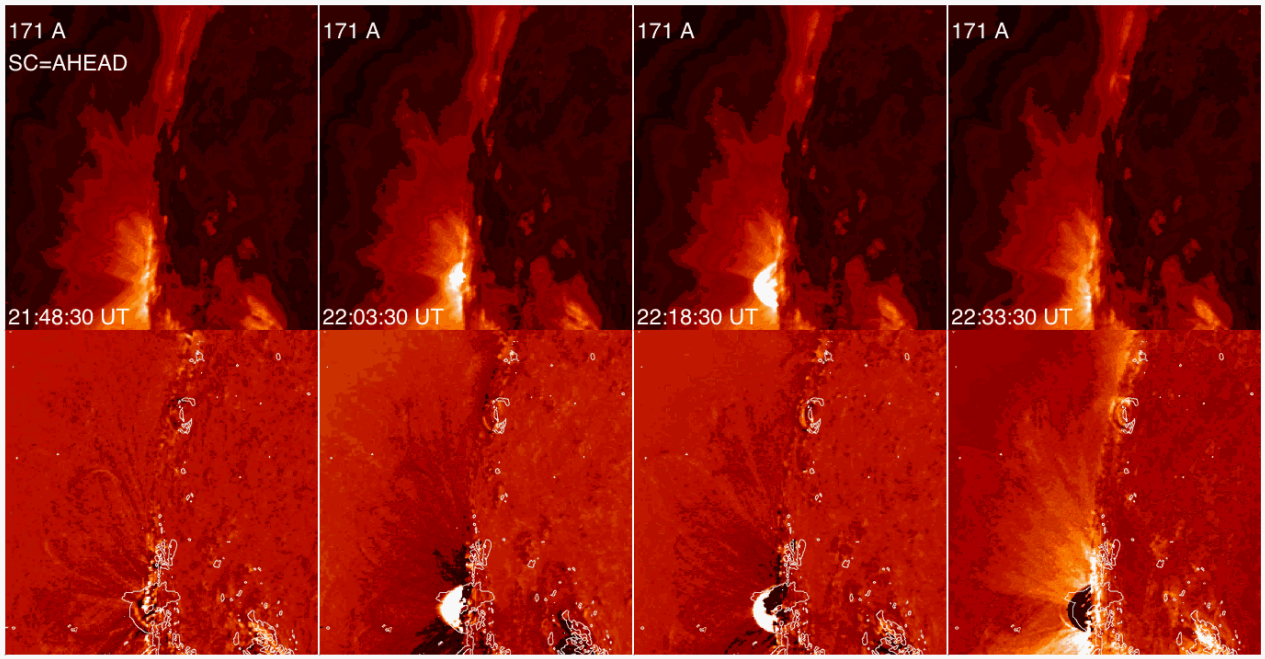

GOES/Hi 0.5-4 A
GOES/Lo 1-8 A
HXR~dF_{GOES}/dt
(RHESSI>25 keV)
EUVI 171 A
EUVI Backgr

EUVI 171 A

EUVI 171 A
Running difference

Event #59: 2007-Jun-01 21:35 UT
- occulted flare
- EUV peaks 4 min after SXR

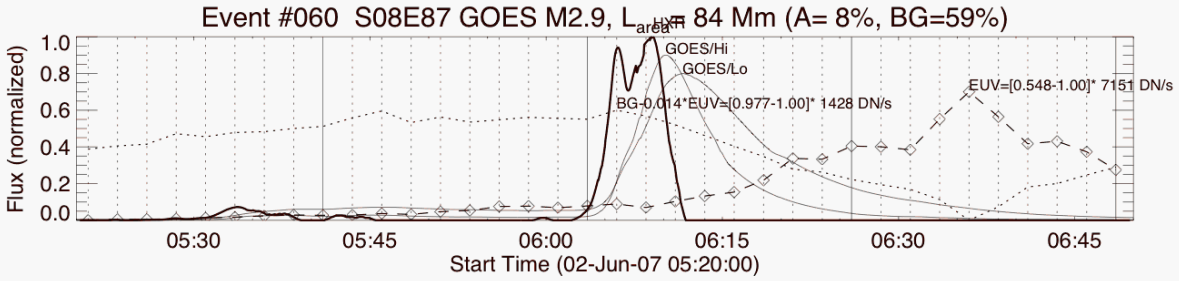

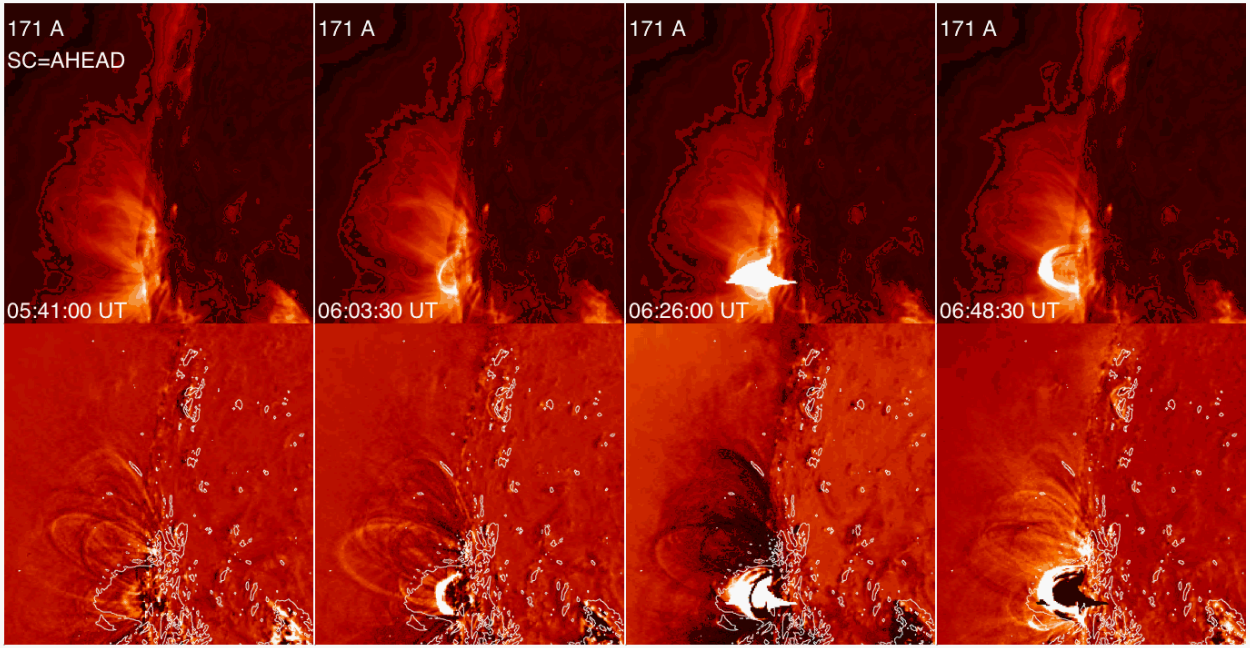

GOES/Hi 0.5-4 A
GOES/Lo 1-8 A
HXR~dF_{GOES}/dt
(RHESSI>25 keV)
EUVI 171 A
EUVI Backgr

EUVI 171 A

EUVI 171 A
Running difference

Event #60: 2007-Jun-02 06:00 UT

- flare near East limb, postflare arcade side-on view
- EUV peaks 30 min after SXR

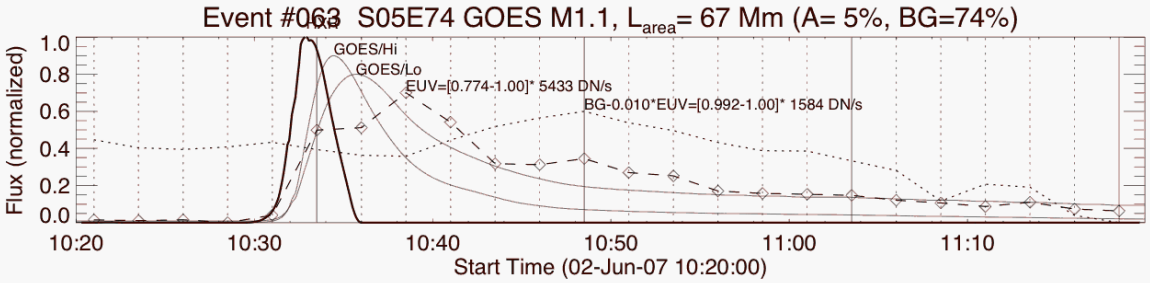

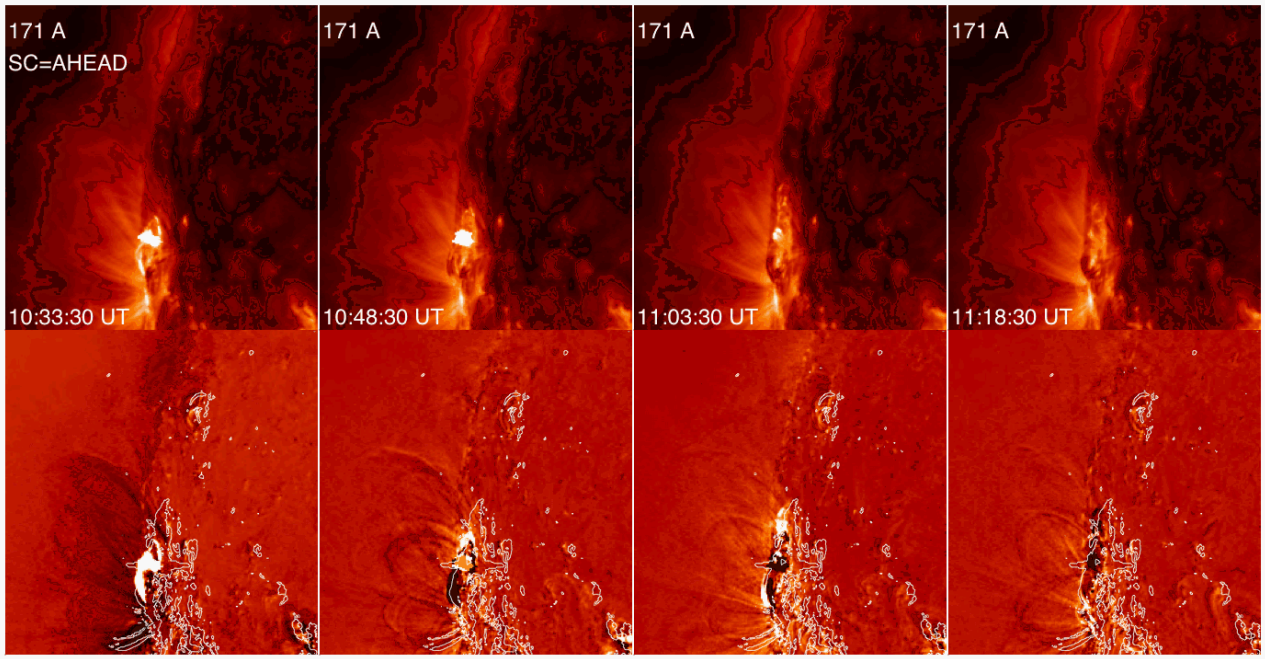

GOES/Hi 0.5-4 A
GOES/Lo 1-8 A
HXR~dF$_{GOES}$/dt
(RHESSI>25 keV)
EUVI 171 A
EUVI Backgr

EUVI 171 A

EUVI 171 A
Running difference

Event #63: 2007-Jun-02 10:30 UT

- flare near East limb, very compact
- EUV peaks 4 min after SXR

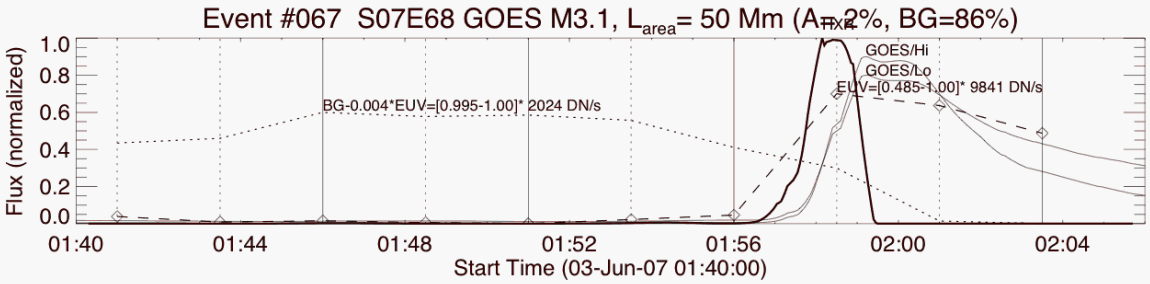

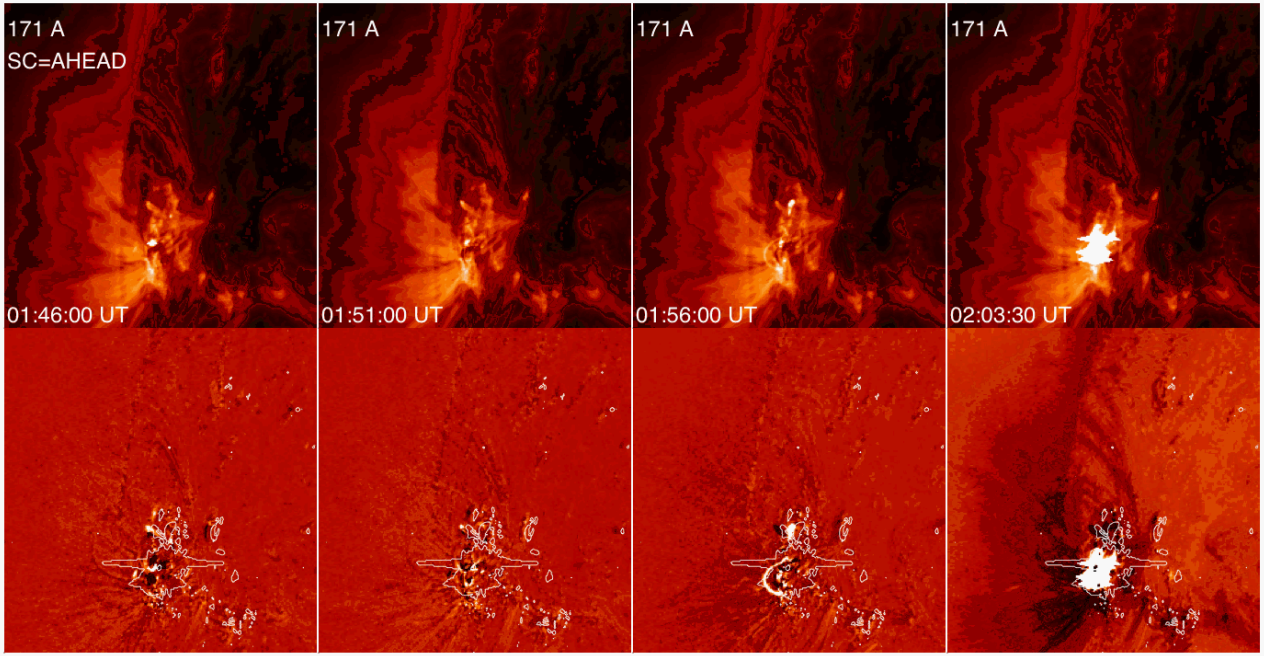

GOES/Hi 0.5-4 A
GOES/Lo 1-8 A
HXR~dF$_{GOES}$/dt
(RHESSI>25 keV)
EUVI 171 A
EUVI Backgr

EUVI 171 A

EUVI 171 A
Running difference

Event #67: 2007-Jun-03 01:56 UT
- flare E70, compact
- EUV peaks simultaneous with SXR

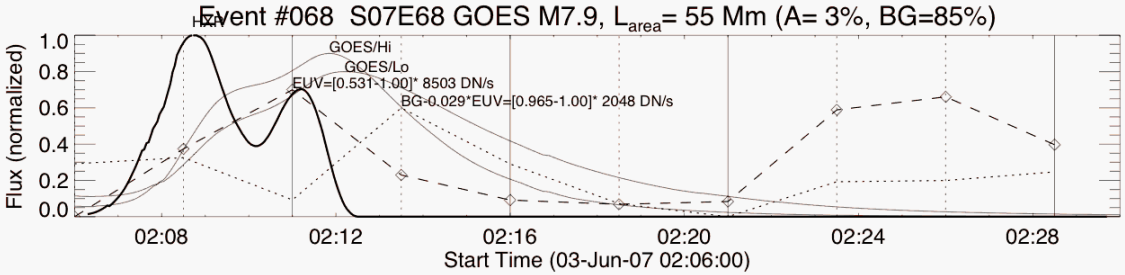

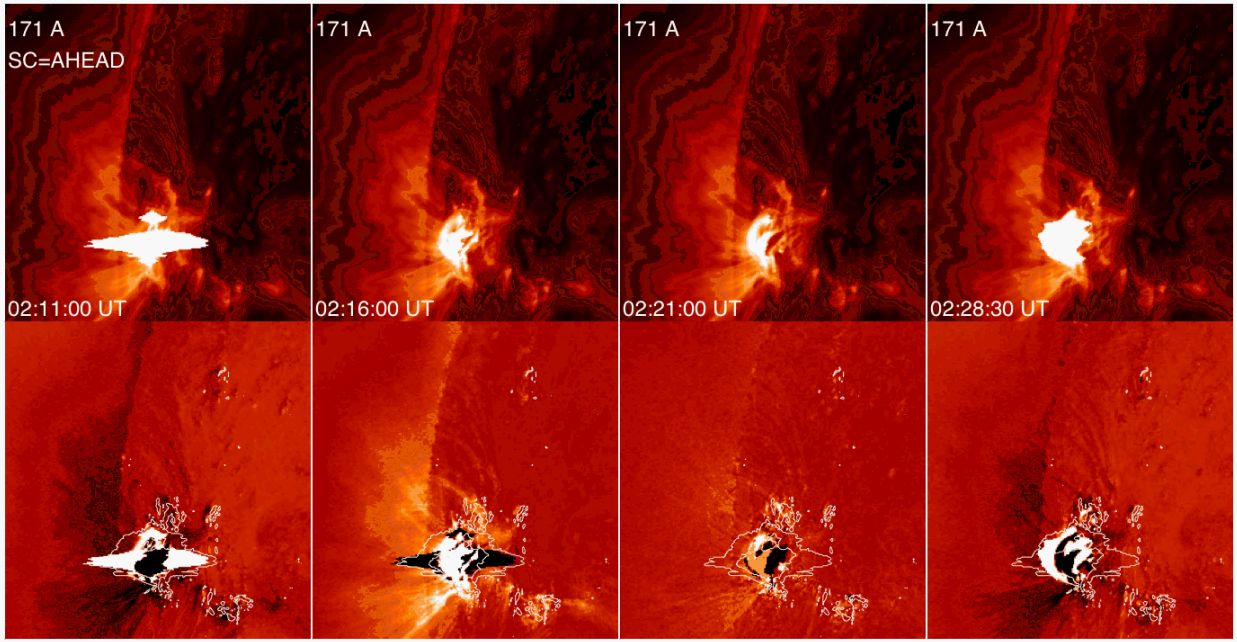

GOES/Hi 0.5-4 A
GOES/Lo 1-8 A
HXR~dF_{GOES}/dt
(RHESSI>25 keV)
EUVI 171 A
EUVI Backgr

EUVI 171 A

EUVI 171 A
Running difference

Event #68: 2007-Jun-03 02:08 UT
- flare E70, postflare arcade
- EUV peaks simultaneously and 16 min after SXR

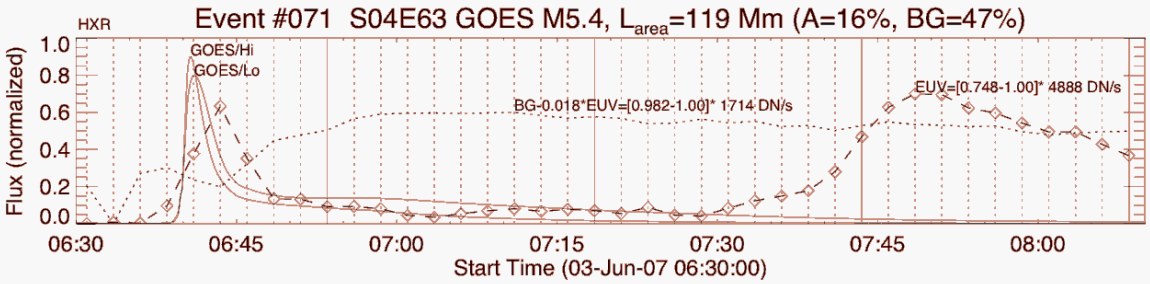

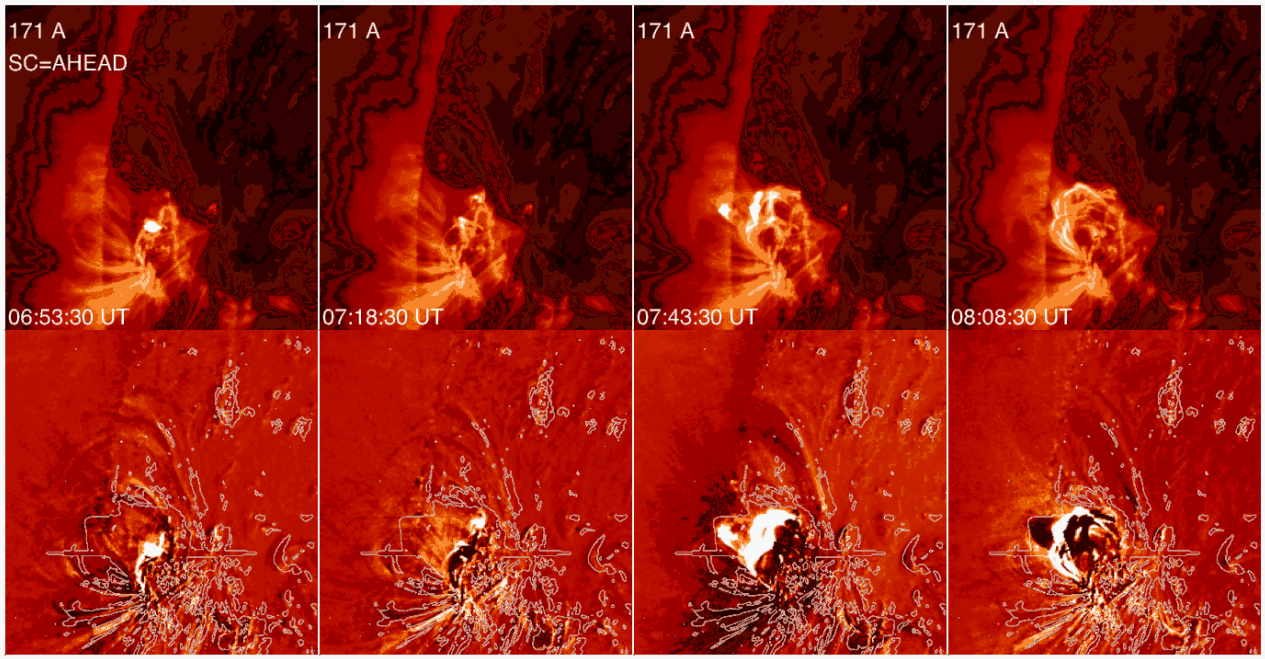

GOES/Hi 0.5-4 A
GOES/Lo 1-8 A
HXR~dF$_{GOES}$/dt
(RHESSI>25 keV)
EUVI 171 A
EUVI Backgr

EUVI 171 A

EUVI 171 A
Running difference

Event #71: 2007-Jun-03 06:30 UT

- flare E63, complex postflare arcade with twisted loops
- EUV peaks simultaneously with SXR and 65 min later !!!

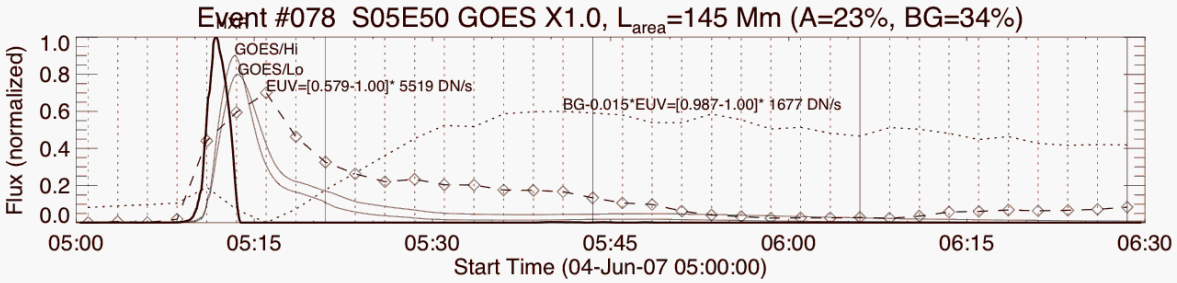

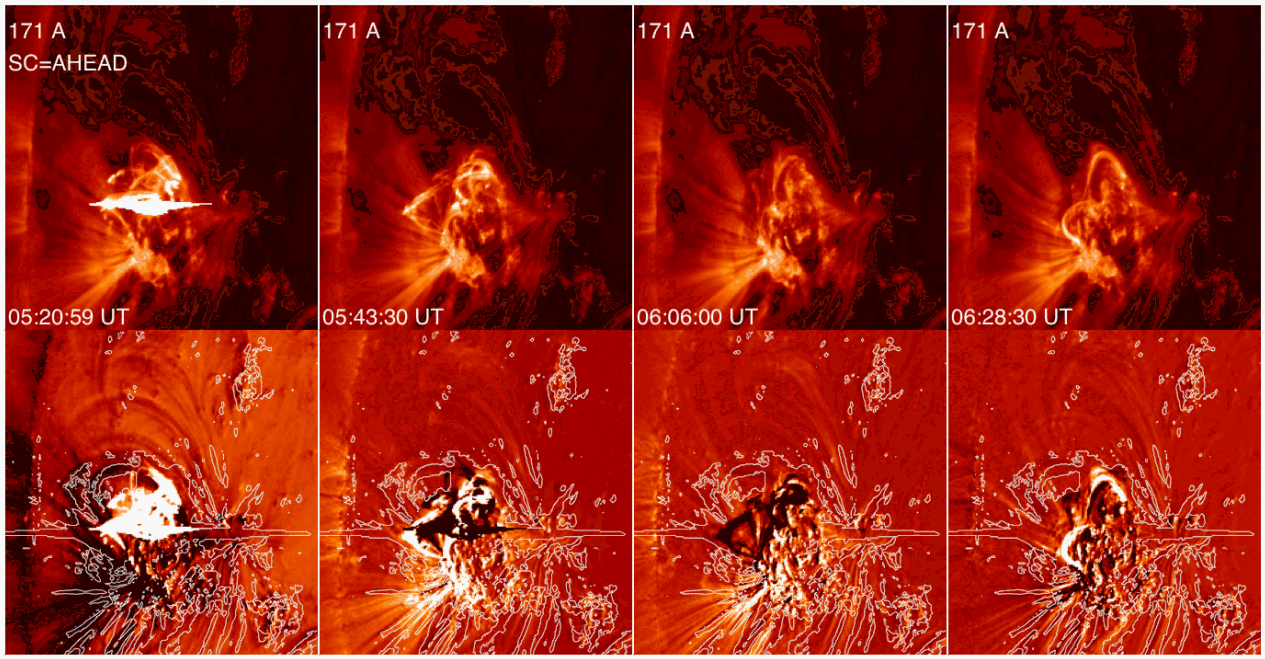

GOES/Hi 0.5-4 A
GOES/Lo 1-8 A
HXR~dF_{GOES}/dt
(RHESSI>25 keV)
EUVI 171 A
EUVI Backgr

EUVI 171 A

EUVI 171 A
Running difference

Event #78: 2007-Jun-04 05:10 UT

- flare E50, complex postflare arcade with twisted loops
- EUV peaks 2 min after SXR

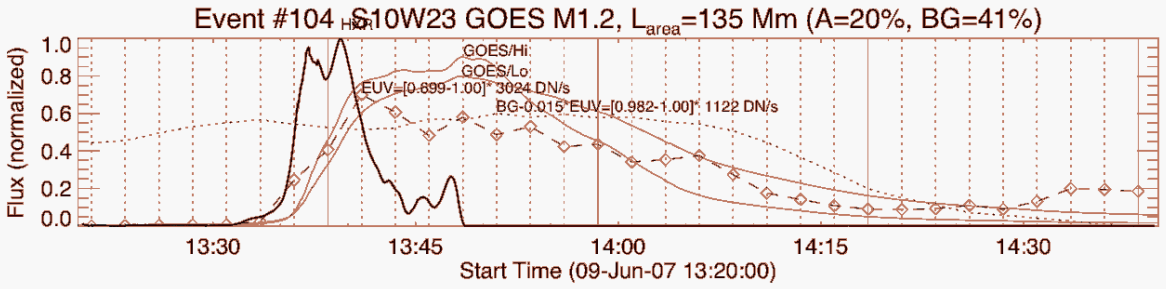

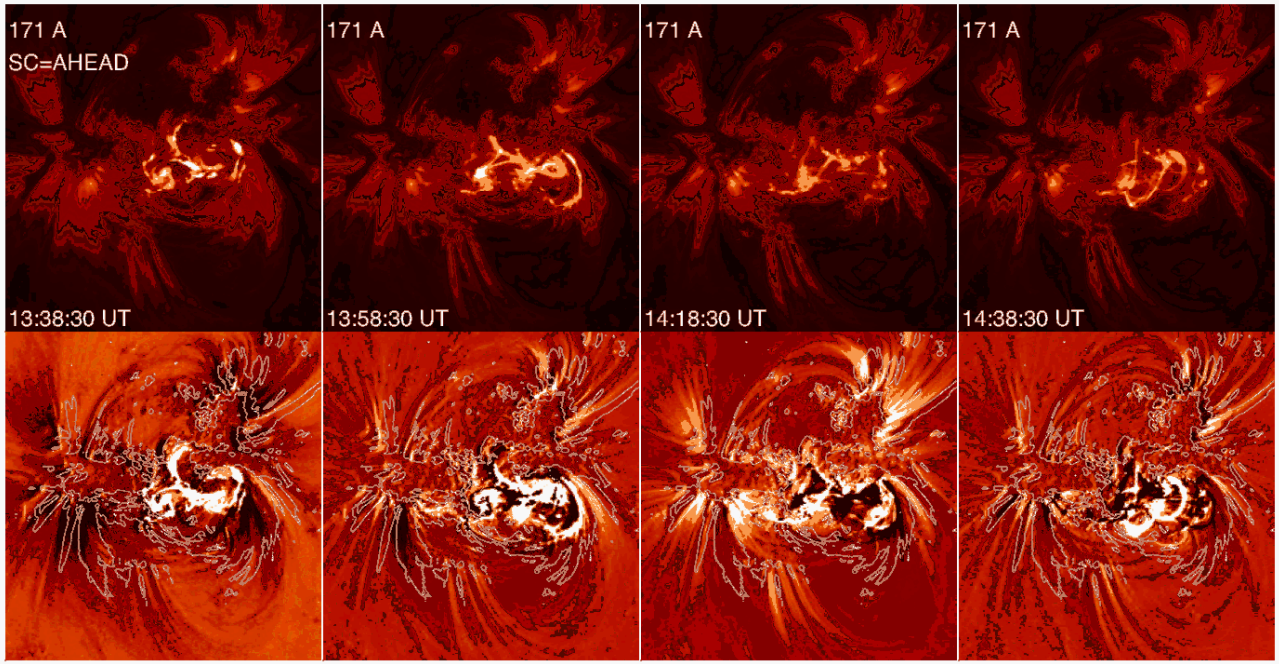

GOES/Hi 0.5-4 A
GOES/Lo 1-8 A
HXR~dF$_{GOES}$/dt
(RHESSI>25 keV)
EUVI 171 A
EUVI Backgr

EUVI 171 A

EUVI 171 A
Running difference

Event #104: 2007-Jun-09 13:30 UT

- flare W23, complex twisted postflare arcade
- EUV not delayed to SXR !!!

Hydrodynamic Modeling: Motivation

-EUV is generally delayed to SXR as a consequence of the flare plasma cooling from ~10 MK down to 1 MK Can we use the SXR-EUV delay to measure the cooling time and derive physical parameters?

-The SXR and EUV light curves constrain the temperature and density evolution of flare loops. Can we infer the heating function (heating rate, duration, scale height) of the flare and determine the total deposited energy?

-How is the thermal energy of a flare related to the available free magnetic energy and the CME energy?

Time-dependent hydrodynamic equations:

$$\rho \frac{De}{Dt} + p\nabla \mathrm{v} = E_H - E_R - \nabla F_C \,. \tag{4.1.20}$$

The hydrodynamic equations (4.1.2−4) for coronal loops can be written more specifically, in one dimension, with loop coordinate s, by inserting the operator D/Dt explicitly, using $\rho = mn$, and the form (Eq. 4.1.20) of the energy equation,

$$\frac{\partial n}{\partial t} + \frac{\partial}{\partial s}(n\mathrm{v}) = 0 \,, \tag{4.1.21}$$

$$mn\frac{\partial \mathrm{v}}{\partial t} + mn\mathrm{v}\frac{\partial \mathrm{v}}{\partial s} = -\frac{\partial p}{\partial s} + \frac{\partial p_{grav}}{\partial r}\left(\frac{\partial r}{\partial s}\right) \,, \tag{4.1.22}$$

$$mn\frac{\partial e}{\partial t} + mn\mathrm{v}\frac{\partial e}{\partial s} + p\frac{\partial \mathrm{v}}{\partial s} = E_H - E_R - \frac{\partial F_C}{\partial s} \,. \tag{4.1.23}$$

The hydrodynamic equations can be generalized for a variable cross-sectional area $A(s)$. The operator (4.1.1) for the total derivative can be transformed (in 3D) into a coordinate system that follows the loop coordinate s, with $\mathrm{v}(s)$ being the parallel velocity. Integrating the flux quantities over the perpendicular cross-sectional area $\int dA(s)$ and dividing the equations by the cross section $A(s)$ then yields

$$\frac{\partial n}{\partial t} + \frac{1}{A}\frac{\partial}{\partial s}(n\mathrm{v}A) = 0 \,, \tag{4.1.24}$$

$$mn\frac{\partial \mathrm{v}}{\partial t} + mn\mathrm{v}\frac{\partial \mathrm{v}}{\partial s} = -\frac{\partial p}{\partial s} + \frac{\partial p_{grav}}{\partial r}\left(\frac{\partial r}{\partial s}\right) \,, \tag{4.1.25}$$

$$mn\frac{\partial e}{\partial t} + \frac{mn\mathrm{v}}{A}\frac{\partial}{\partial s}(eA) + \frac{p}{A}\frac{\partial}{\partial s}(\mathrm{v}A) = E_H - E_R - \frac{1}{A}\frac{\partial}{\partial s}(F_C A) \,. \tag{4.1.26}$$

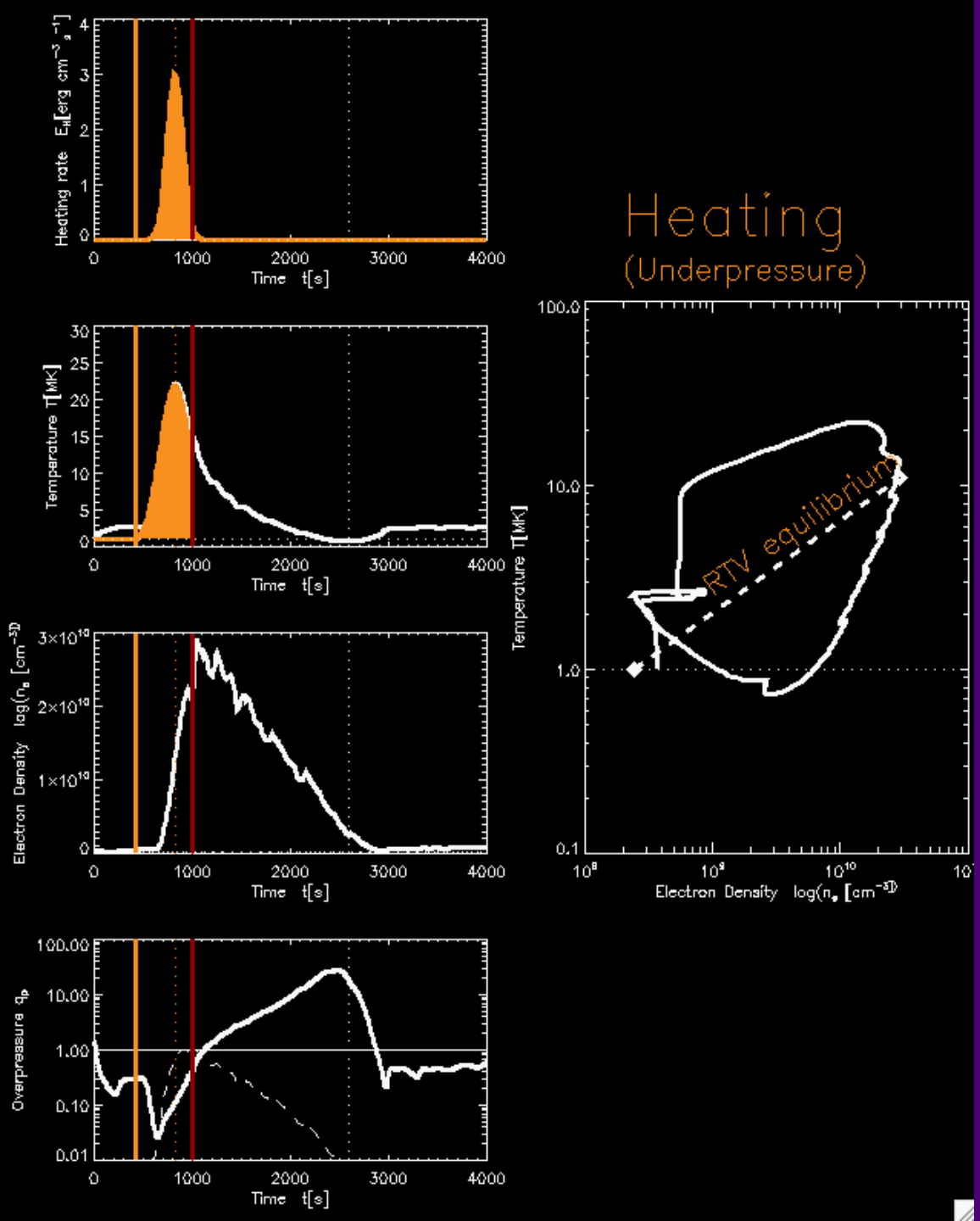

The temperature evolution T(t) of the heating phase can be analytically described from the evolution of the heating function (neglecting radiative loss)

$$E_H(s,t) - \frac{d}{ds}\left[\frac{2}{7}\kappa T(s)^{5/2}\frac{dT}{ds}\right] = \frac{2}{7}\kappa\frac{d^2T^{7/2}(s)}{ds^2}$$

$$E_{Hm} = E_H(t=t_m) \approx 2\kappa\frac{T_m^{7/2}}{L^2}$$

$$T(t<t_m) = \left[\frac{L^2}{2\kappa}E_H(t)\right]^{2/7}$$

Gaussian heating function

$$E_H(t) = E_{Hm}\exp\left(-\frac{(t-t_m)^2}{2\tau_{heat}^{\ 2}}\right)$$

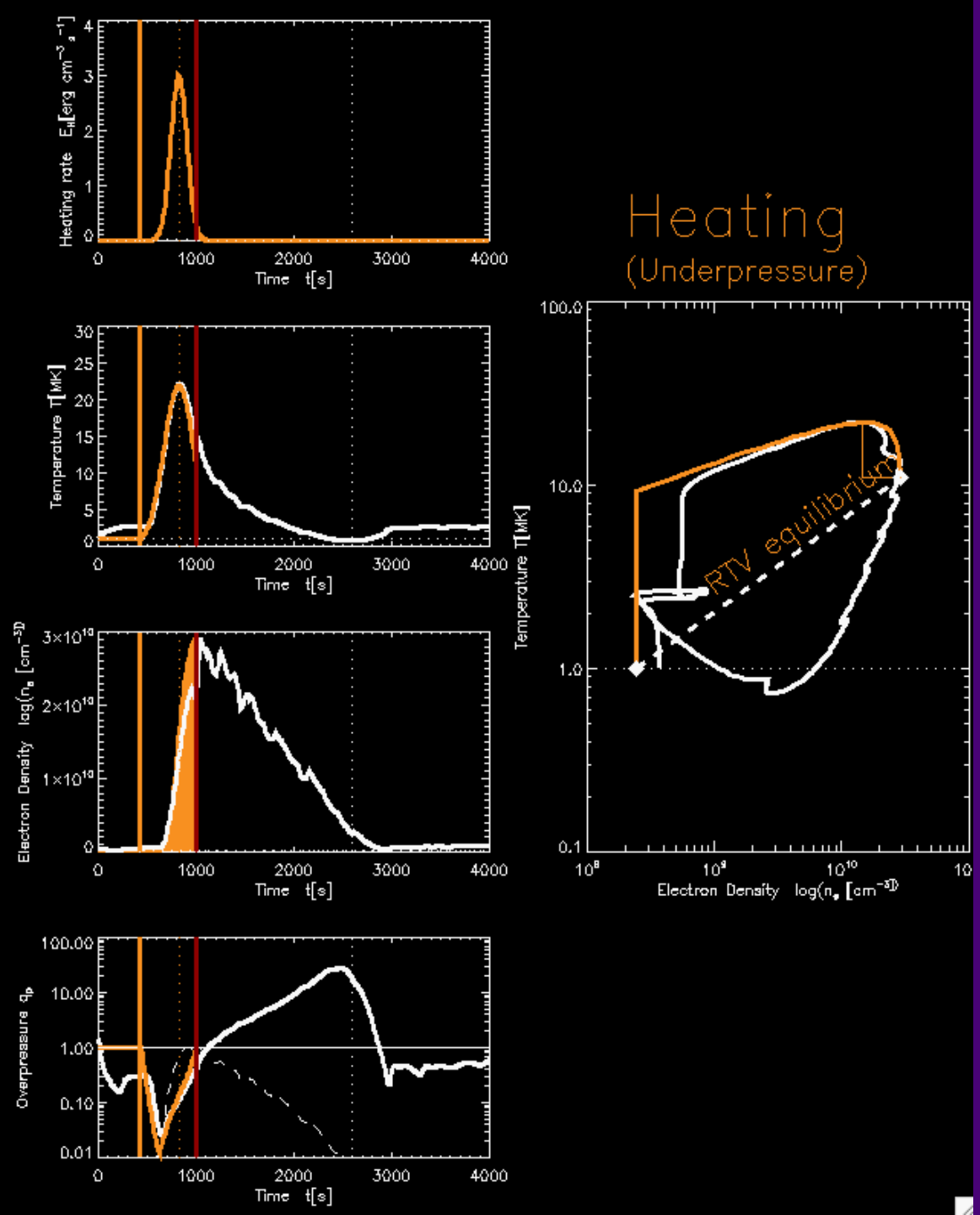

The electron density evolution n(t) of the heating phase can be analytically described with the Neupert effect: the density increases with the time integral of the evaporation rate (=heating rate)

$$n(t) \propto \int_0^t \left(\frac{E_H(t)}{E_{Hm}} \right) dt', t < t_p$$

$$n_p = n(t = t_p)$$

$$n_m = n(t = t_m) = n_p \frac{T_p}{T_m} = \frac{n_p}{2}$$

$$p \propto n_m T_m \approx n_p T_p$$

Pressure approximately constant near peak time

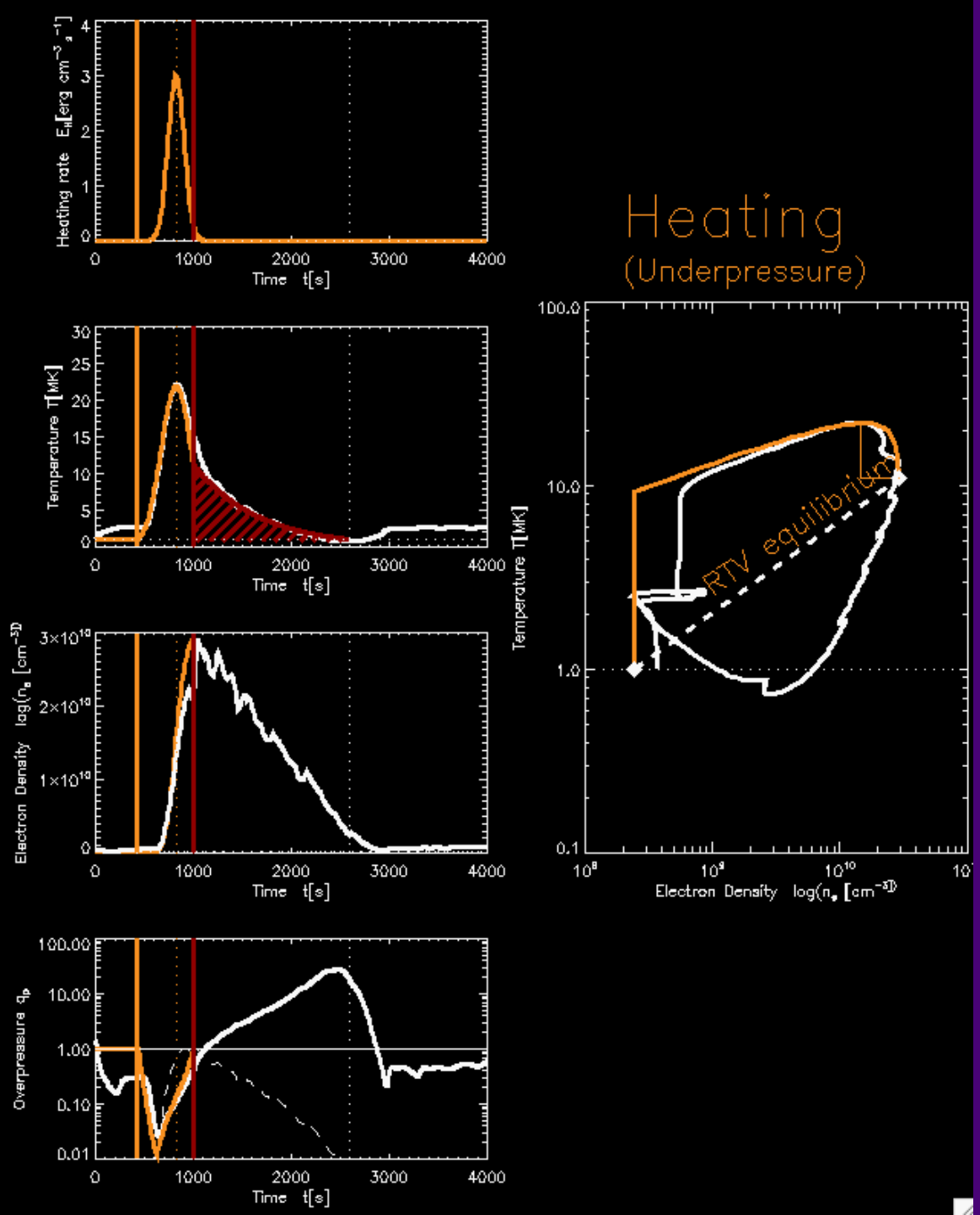

The temperature evolution T(t) in the cooling phase is Initially dominated by thermal conduction, and later by radiative loss (for low densities or low temperatures)

$$T(t) = T_p \exp(-\frac{(t - t_p)}{\tau_{cool}}), t > t_p$$

$$\frac{1}{\tau_{cool}} = \frac{1}{\tau_{cond}} + \frac{1}{\tau_{rad}},$$

$$\tau_{cool} \approx \frac{1}{2}\tau_{cond},$$

$$\tau_{cond} = \frac{21}{5}\frac{n_p k_B L^2}{\kappa T^{5/2}}$$

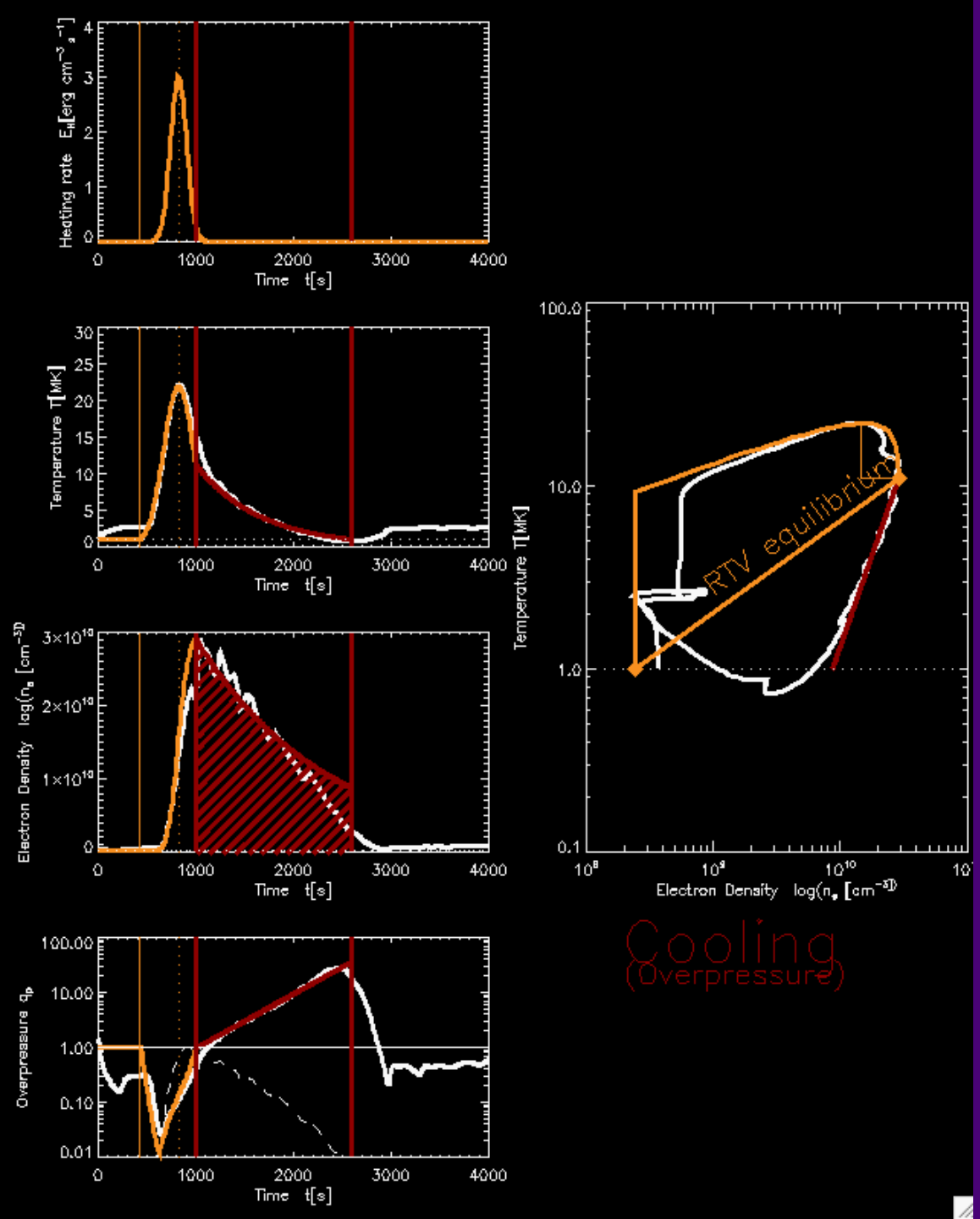

The electron density evolution n(t) in the cooling phase is related to the temperature evolution T(t) by a powerlaw function (Jakimiec relation)

$$\frac{n(t)}{n_p} = \left(\frac{T(t)}{T_p}\right)^a,$$

$$a \approx 2$$

$$n(t) = n_p \exp\left(-\frac{(t - t_p)}{\tau_{drain}}\right),$$

$$\tau_{drain} \approx a\,\tau_{cool} \approx 2\,\tau_{cool}$$

Analytical code that approximates hydrodynamic evolution of heated and cooling flare loops (Aschwanden & Tsiklauri 2008)

the *heating non-uniformity factor* q_H (Eq. 21),

$$q_H = \frac{(L/s_H)^2}{2[1-(1+L/s_H)\exp(-L/s_H)]} \ , \tag{60}$$

the *maximum apex temperature* $T_m = T(s=L, t=t_m)$ (Eq. 25),

$$T_m = \left[\frac{7L^2H_0}{4\kappa\ q_H}\right]^{2/7} \ , \tag{61}$$

the *apex temperature* $T_p = T(s=L, t=t_p)$ at the density peak time (Eq. 30),

$$T_p = \frac{T_m}{2} \ , \tag{62}$$

the *Mach number* M (Eq. 43) at the loop apex and density peak time,

$$M \approx 0.32 \left[1 + 0.3\ \arctan\left(\frac{L}{2s_H}\right)\right]\left[1 + 2.65 \exp\left(-\frac{(H_{max}+2.5\tau_{heat})}{200}\right)\right] \ , \tag{63}$$

the corresponding *sound speed* c_s (Eq. 39) at the loop apex and maximum heating time t_m,

$$c_s = c_{s0}\left(\frac{T_m}{\mu}\right)^{1/2} \ , \tag{64}$$

the loop apex *electron density* $n_m = n(s=L, t=t_m)$ at the time of the temperature maximum (Eq. 42),

$$n_m = \frac{H_0 s_H [1-\exp(-\frac{L}{s_H})]}{M c_s [\frac{5}{2} k_B T_m + \frac{1}{2} m_p (M c_S)^2 - m_p g_\odot L \frac{2}{\pi}]} \ , \tag{65}$$

the *peak electron density* $n_p = n(s=L, t=t_p)$ (Eq. 28) at the loop apex,

$$n_p = 2\ n_m \ . \tag{66}$$

If we choose the time $t = t_m$ of maximum heating as the reference time, and a coronal background temperature T_0, say $T_0 = 1.0$ MK, we obtain the start time t_s (Eq. 26),

$$t_s = t_m - \tau_{heat}\sqrt{7\ \ln(T_m/T_0)} \ , \tag{67}$$

the *density peak time* t_p (Eq. 31),

$$t_p = t_m + \tau_{heat}\sqrt{7 \ln 2} \ , \tag{68}$$

and the *end time* t_e (Eq. 57),

$$t_e = t_p + \tau_{cool}\sqrt{2\ \ln(T_p/T_0)} \ . \tag{69}$$

Furthermore we have five particular time scales: the *evaporation time scale* τ_{evap} (Eq. 33),

$$\tau_{evap} = \sqrt{7/2}\ \tau_{heat} \ , \tag{70}$$

the *conductive cooling time* τ_{cond} at the density peak time (Eq. 46),

$$\tau_{cond} = \frac{21}{5}\frac{n_p k_B L^2}{\kappa T_p^{5/2}} \ . \tag{71}$$

the *radiative cooling time* τ_{rad} at the density peak time (Eq. 51),

$$\tau_{rad} = \frac{9 k_B T_p^{5/3}}{5 n_p \Lambda_0} \ . \tag{72}$$

the combined *cooling time scale* τ_{cool} (Eq. 53),

$$\tau_{cool} = \frac{1}{2}\left[\frac{1}{\tau_{cond}} + \frac{1}{\tau_{rad}}\right]^{-1} \ , \tag{73}$$

and the *draining time scale* τ_{drain} (Eq. 56),

$$\tau_{drain} = 2\ \tau_{cool} \ . \tag{74}$$

Now we have all parameter constants to express the evolution of the temperature profile $T(s=L,t)$ at the loop apex (Eqs. 24, 52),

$$T(s=L,t) = \begin{cases} T_m \left[\exp\left(-(t-t_m)^2/2\tau_{heat}^2\right)\right]^{2/7} & \text{for } t \le t_p \\ T_p\ \exp\left(-(t-t_p)^2/2\tau_{cool}^2\right) & \text{for } t > t_p \end{cases} \ , \tag{75}$$

and the evolution of the density profile $n(s=L,t)$ at the loop apex (Eqs. 32, 55),

$$n(s=L,t) = \begin{cases} n_p\ \exp\left(-(t-t_p)^2/2\tau_{evap}^2\right) & \text{for } t \le t_p \\ n_p\ \exp\left(-(t-t_p)^2/2\tau_{drain}^2\right) & \text{for } t > t_p \end{cases} \ . \tag{76}$$

The spatial profiles can be approximated with equilibrium solutions if significant changes in density occur slower than the sound travel time along the loop, since density gradients due to dynamic processes are smoothed out by pressure adjustments that propagate with the sound speed. The spatial loop profile is then according to the solution given in Eq. (22) and the loop apex evolution $T(s=L,t)$ given in Eq. (22),

$$T(s,t) = T(s=L,t)\left[\left(\frac{s}{L}\right) + 2q_H\left(\frac{s_H}{L}\right)^2\left(1-\exp\left(-\frac{s}{s_H}\right) - \left(\frac{s}{L}\right)\left[1-\exp\left(-\frac{L}{s_H}\right)\right]\right)\right]^{2/7} \ . \tag{77}$$

The pressure or density scale height λ_p of hydrostatic loops is a function of the temperature, for which we can use approximately the expression for the apex temperature $T(s=L,t)$,

$$\lambda_p(T[t]) = \frac{2k_B T(s=L,t)}{\mu m_H g_\odot} \approx 4.7 \times 10^9 \left(\frac{T(s=L,t)}{1\ \text{MK}}\right)\ \text{cm} \ . \tag{78}$$

The spatial density profile along the loop can be expressed approximately as a function of the loop apex density evolution $n(s=L,t)$ (Eq. 76),

$$n(s,t) = n(s=L,t)\ \exp\left(-\frac{(s-L)}{\lambda_p(T[t])}\right) \ . \tag{79}$$

This set of analytical equations (59-79) provides then an complete approximation to the spatio-temporal evolution of loop temperatures $T(s,t)$ and loop densities $n(s,t)$. The validity range of this analytical code is limited to loop apex temperatures in the coronal range of $T_m \gtrsim 1.0$ MK.

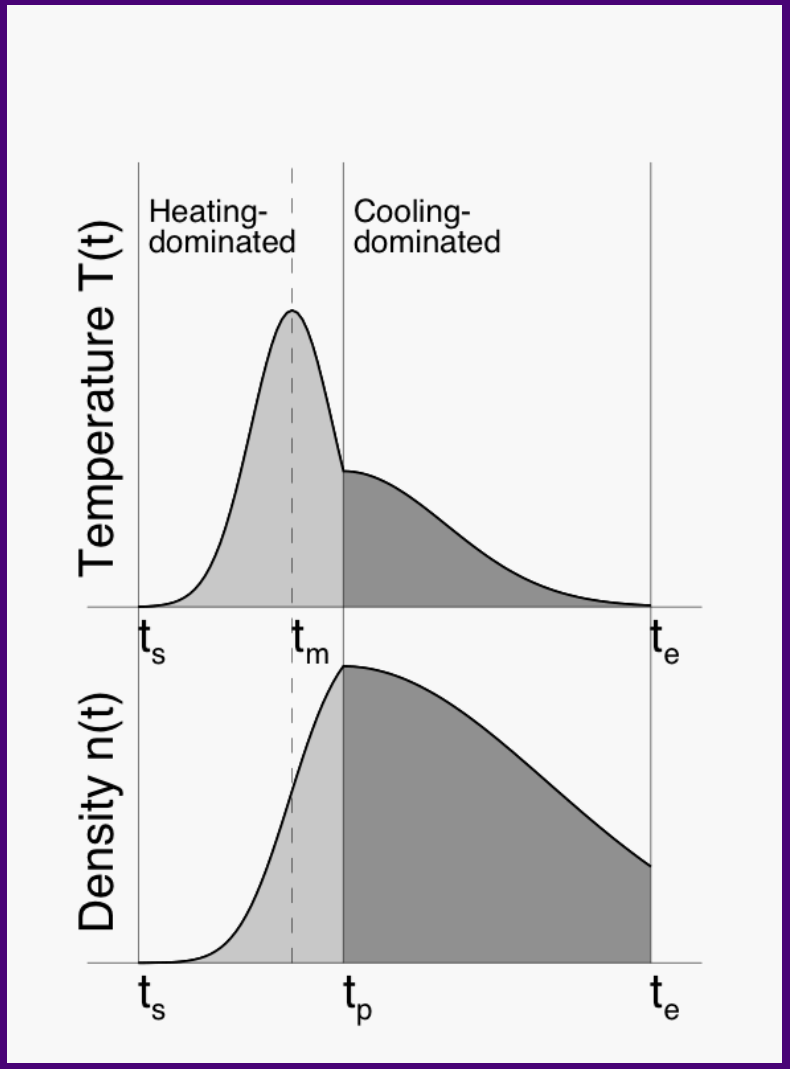

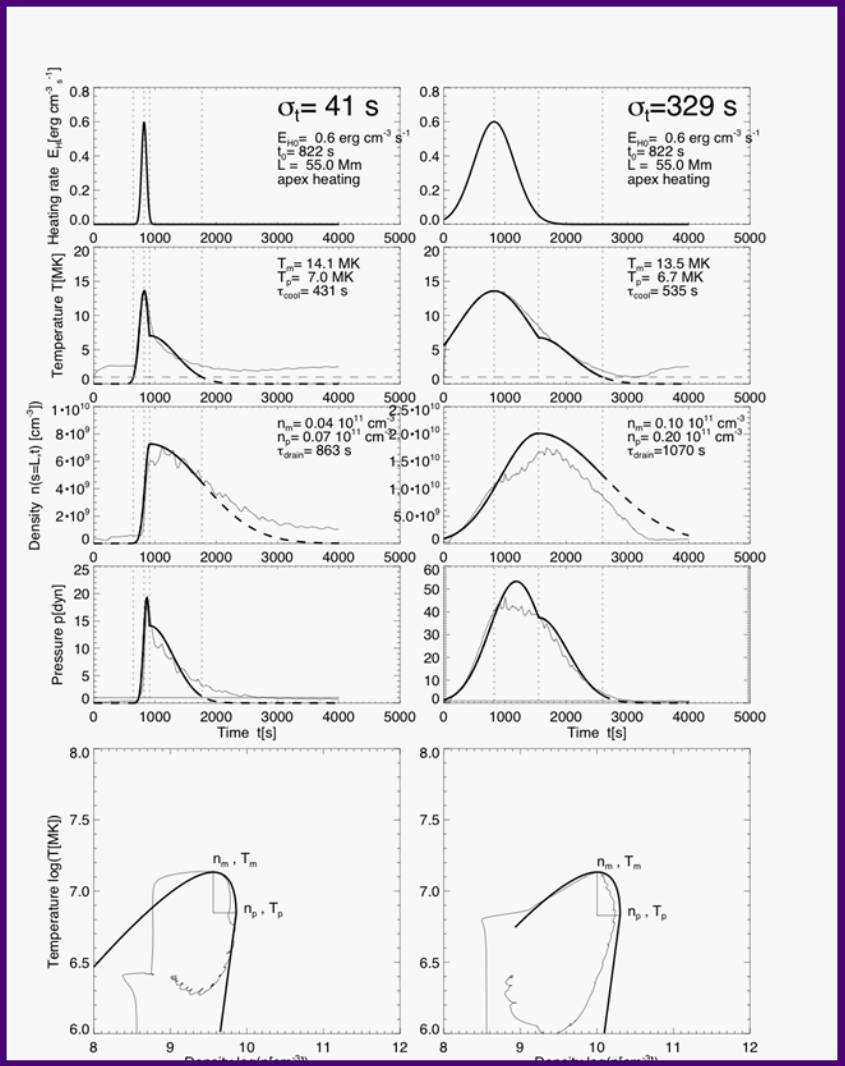

Analytical code is formulated explicitely as a function of heating function (heating rate, heating time scale, heating scale height, & loop length) and is consistent with numerical hydrodynamic simulations (T<5%, n<10%)

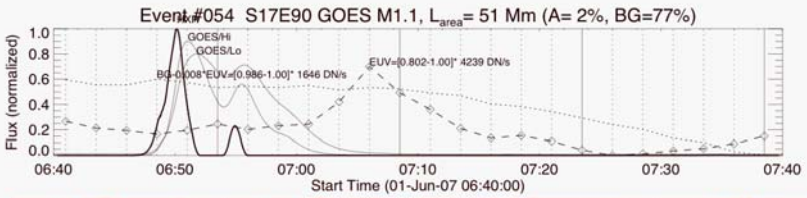

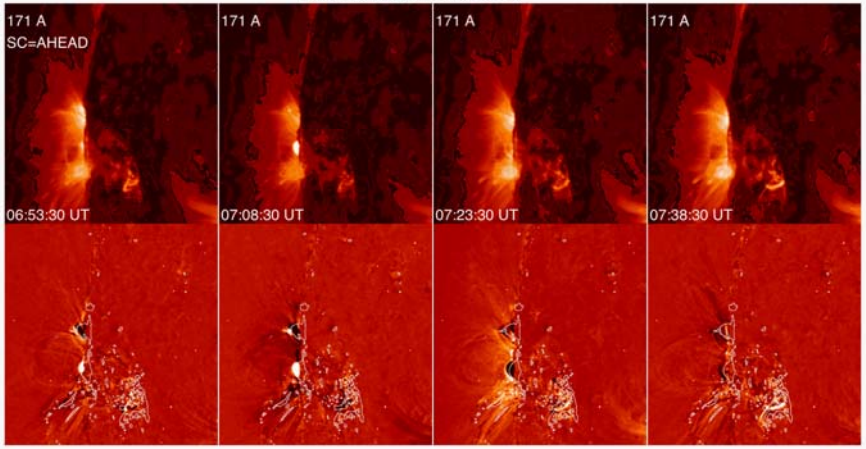

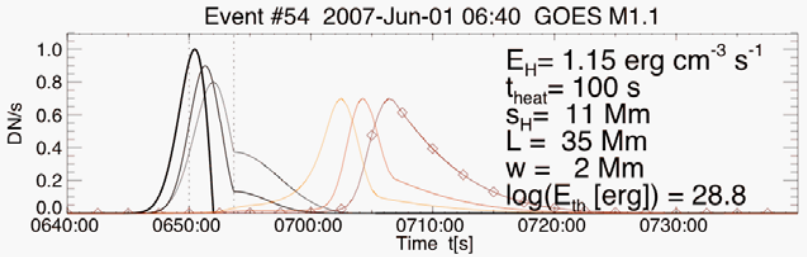

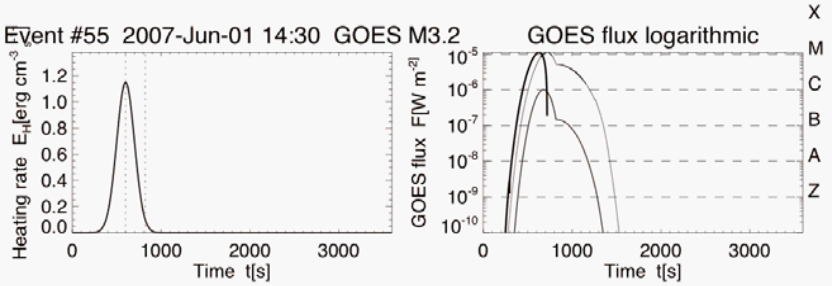

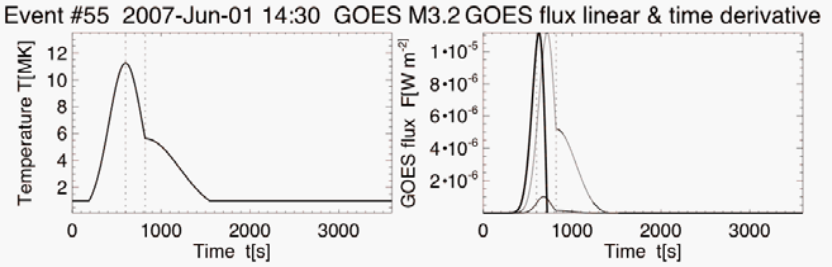

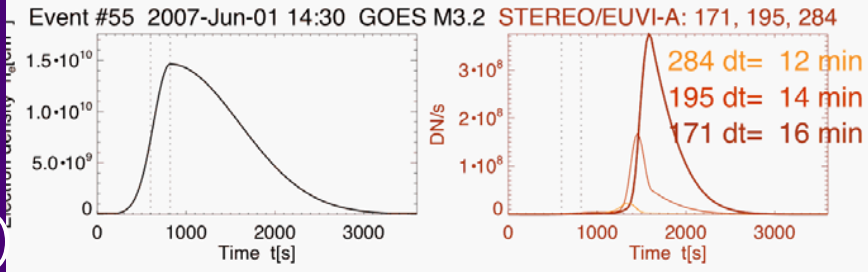

Analytical code matches:

- GOES M1.1 flux
- SXR-EUV delay = 16 min
- Loop length L=35 Mm

Inference of: (T=12 MK, n=1.5*10^{10} cm^{-3})

- Heating rate = 1.15 erg cm^{-3} s^{-1}
- Total thermal energy = $10^{28.8}$ erg

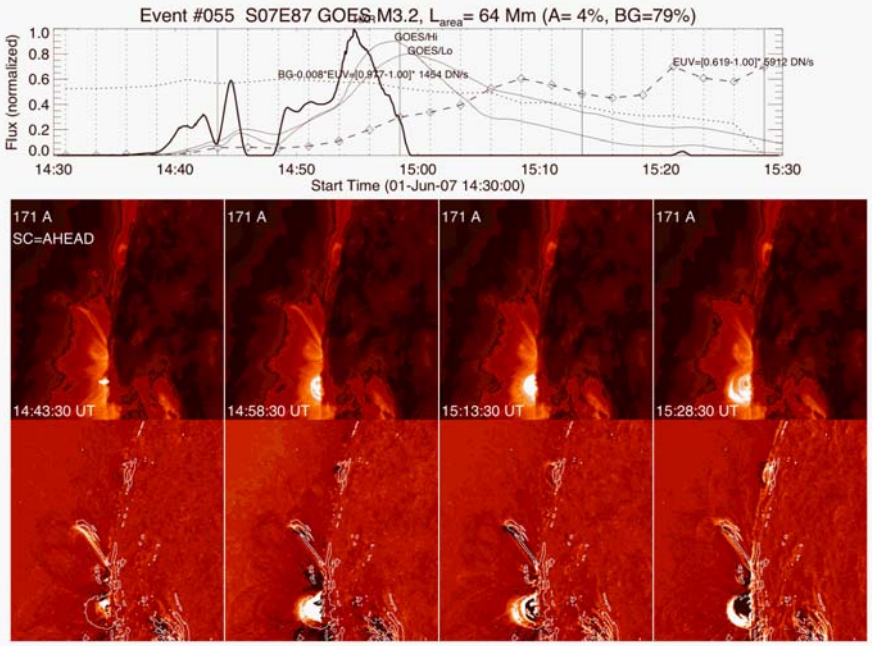

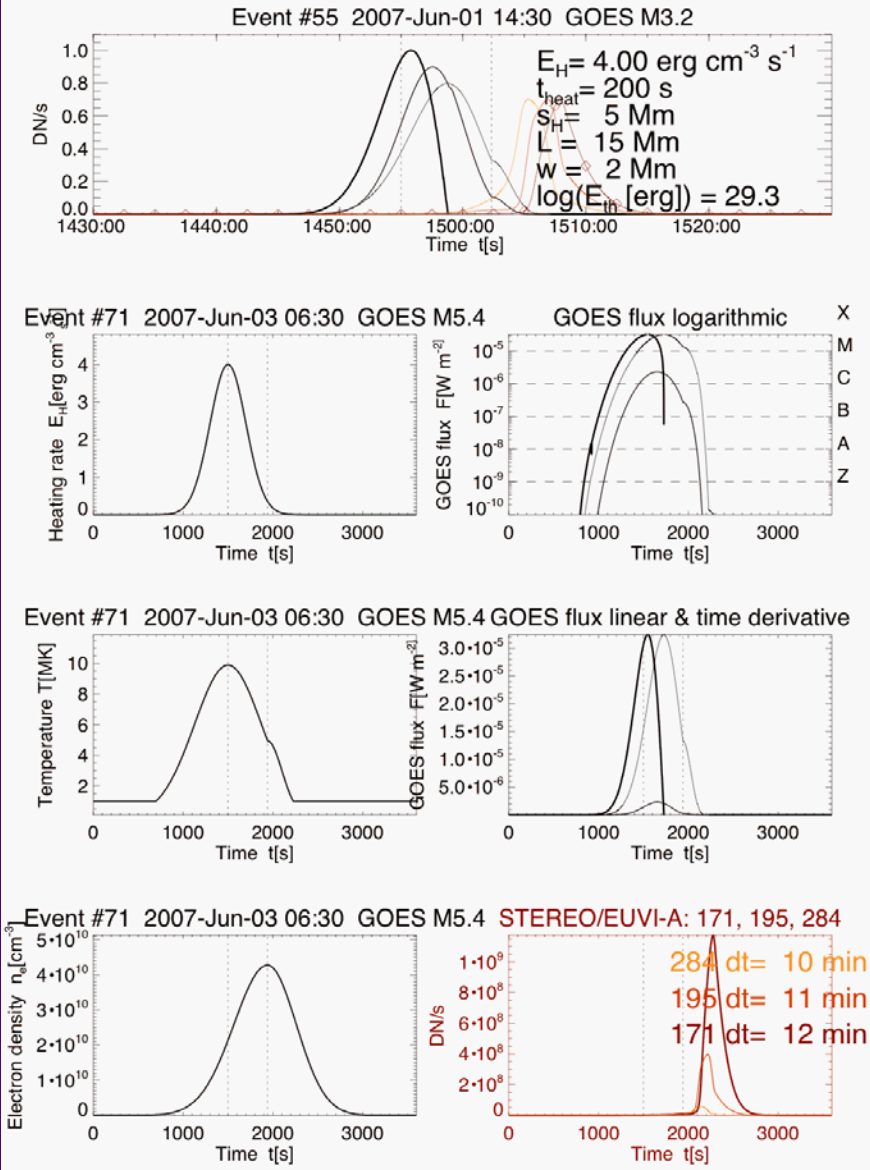

Analytical code matches:

- GOES M3.2 flux
- SXR-EUV delay = 12 min
- Loop length L=15 Mm

Inference of: (T=10 MK, n=4*10^{10} cm^{-3})

- Heating rate = 4.0 erg cm^{-3} s^{-1}
- Total thermal energy = $10^{29.3}$ erg

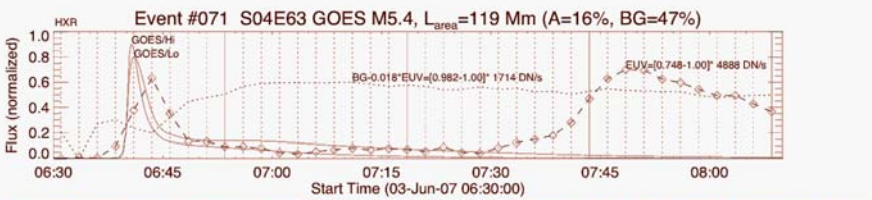

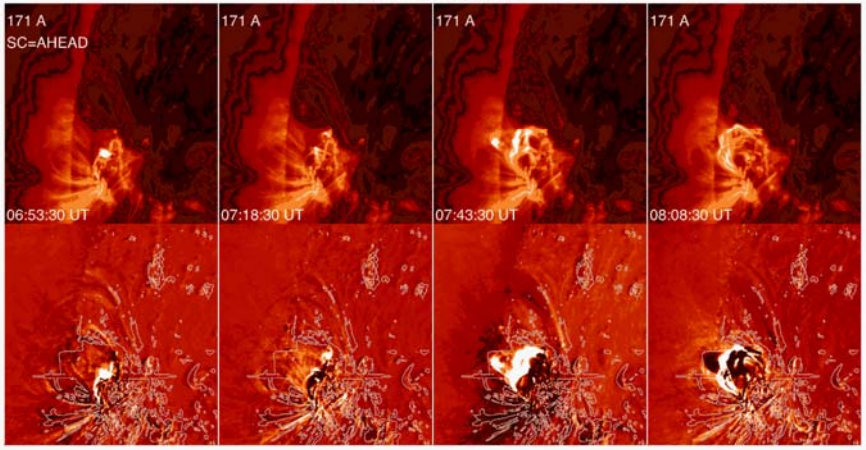

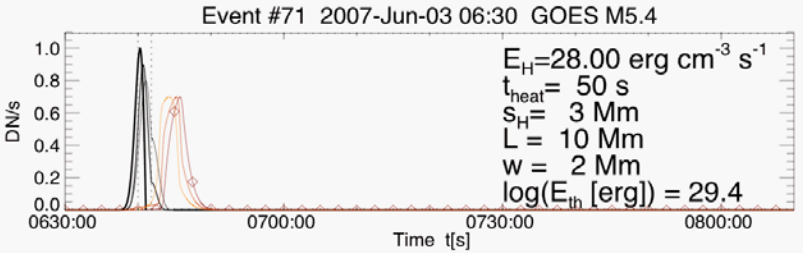

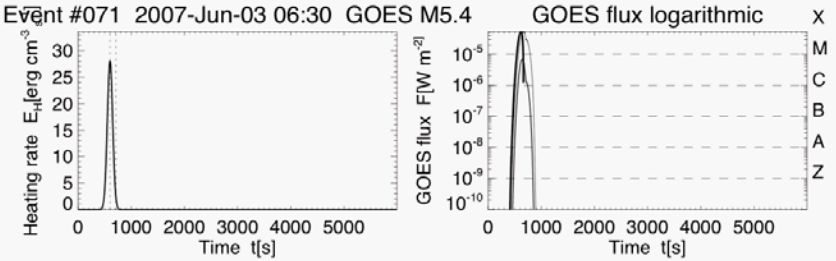

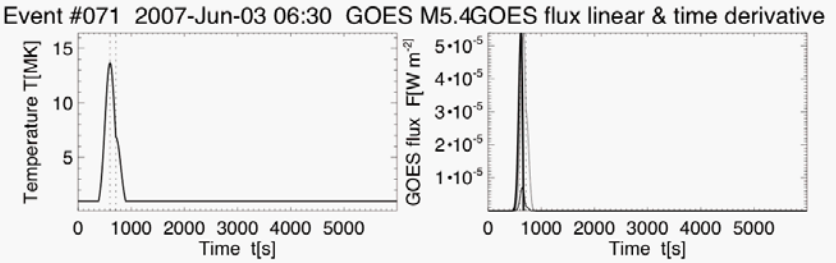

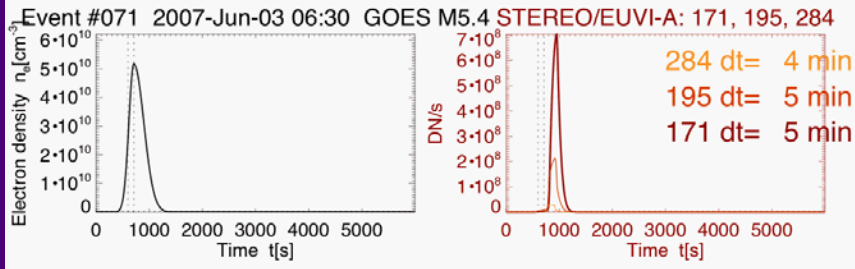

Analytical code matches:

- GOES M5.4 flux
- SXR-EUV delay = 5 min (70 min ?)
- Loop length L=10 Mm

Inference of: (T=14 MK, n=5*10^{10} cm^{-3})

- Heating rate =28.0 erg cm^{-3} s^{-1}
- Total thermal energy = $10^{29.4}$ erg

Conclusions :

(1) Stereoscopy provides 3D geometric parameters (loop lengths, loop widths, flare volume) to constrain loop models and total emission measure of flares.

(2) HXR (RHESSI), soft X-ray (GOES), and EUV (EUVI A+B) light curves constrain temperature T(s) and density n(t) models of the hydrodynamic evolution of flares. Large EUV delays (>1 hr) require expansion of low-density flare plasmas.

(3) New code with analytical approximations to hydrodynamic evolution of heated and cooling loops (Aschwanden & Tsiklauri 2008) allows to infer heating function (E_H, t_H, s_H) and total thermal energy of flare plasma (E_{th}).

(4) Time histories of EUV emission around flare regions reveal dimming in large flares, which can be modeled in 3D to estimate the mass of CMEs.